



HAL
open science

Extension of Beremin model to bi-modal brittle failure

Antoine Andrieu, André Pineau, David Ryckelynck, Olivier Bouaziz

► **To cite this version:**

Antoine Andrieu, André Pineau, David Ryckelynck, Olivier Bouaziz. Extension of Beremin model to bi-modal brittle failure. 20ème Congrès Français de Mécanique, CFM 2011, Aug 2011, Besançon, France. 6 p. hal-00684693

HAL Id: hal-00684693

<https://hal-mines-paristech.archives-ouvertes.fr/hal-00684693>

Submitted on 2 Apr 2012

HAL is a multi-disciplinary open access archive for the deposit and dissemination of scientific research documents, whether they are published or not. The documents may come from teaching and research institutions in France or abroad, or from public or private research centers.

L'archive ouverte pluridisciplinaire **HAL**, est destinée au dépôt et à la diffusion de documents scientifiques de niveau recherche, publiés ou non, émanant des établissements d'enseignement et de recherche français ou étrangers, des laboratoires publics ou privés.

Extension of Beremin model to bi-modal brittle failure

A. Andrieu^a, A. Pineau^a, D. Ryckelynck^a, O. Bouaziz^a

a. Centre des matériaux MinesParitech, UMR CNRS 7633, 10 rue Henry Desbrueres, Corbeil
Essonnes, France

Résumé :

La présence de zones ségréguées dans les aciers utilisés en forte épaisseur a pour effet d'abaisser la ténacité et d'augmenter la dispersion des mesures. Ce comportement s'explique qualitativement par l'observation de poches de rupture intergranulaires dans les zones ségréguées, le reste de la surface étant couvert de facettes de clivage. Le modèle de Beremin, maintenant largement utilisé pour décrire quantitativement la rupture fragile mono mode est étendu au cas bimodal (intergranulaire et clivage). Les prévisions de ce modèle sont confrontées aux mesures expérimentales de ténacité dans un acier renfermant des zones ségréguées.

Abstract :

The presence of segregated zones in steels used in heavy sections leads to both abnormally low values of the fracture toughness and large scatter in test results. This behaviour is explained qualitatively by the existence of a bimodal mode of failure observed on fracture surfaces (intergranular fracture in embrittled segregated zones and cleavage fracture in the matrix). The well-known Beremin model, now largely used to describe quantitatively brittle fracture in the presence of only brittle fracture is extended to account for bimodal failure. This model is compared to experimental results of fracture measurements in segregated materials.

Mots clefs : Beremin model, bimodal fracture, inhomogeneity

1 Introduction

Recent studies have shown that abnormally low values of fracture toughness, K_{JC} , and abnormally large scatter in K_{JC} measurements can be met when testing CT specimens taken from thick steel components [5,14,15]. Similar observations were previously reported by Naudin and al. [8-10] in a large test program led at EDF on CT_{25} specimens taken from a nozzle shell of a nuclear pressurized water reactor (PWR). These authors showed that the abnormally low values of K_{JC} were systematically associated with the presence of segregated zones (SZ) which led to local brittle intergranular fracture instead of cleavage fracture. These SZ's, that arose from the solidification process of thick components, are enriched in both alloying elements (Mn, Ni, Mo) and impurities (P,S). The segregation of these impurities along the prior austenitic grains during heat-treatment triggers intergranular fracture in SZ's. The material can thus be considered as a composite containing brittle SZ's which fail at a lower stress and the matrix which fails by cleavage fracture. The Beremin model has been largely used to describe brittle fracture (see e.g [11]). However this model has not yet been used to account for the presence of inhomogeneities, which is precisely the aim of the present study. The paper is organised as follows. After a brief presentation of the properties of SZ's, a new bimodal Beremin type model is presented. The predictions obtained from this model are compared to the experimental results from a large test program run at EDF.

2 Materials and experimental results

Position of the problem : The material analysed in this study is a A508 class3 steel taken from a thick PWR shell. Fig.1a shows that the SZ's are preferentially located close to the inner side of the vessel. A schematic representation of the SZ's distribution as well as the position of the fracture toughness specimens is shown in Fig.1b. Chemical analysis of the SZ's revealed a strong segregation

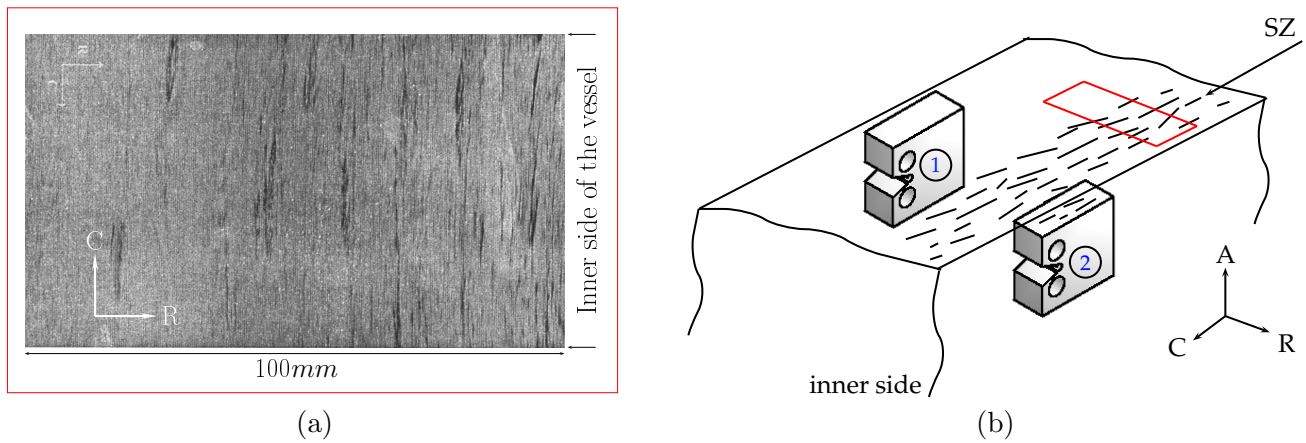


FIG. 1 – (a) : View of a slice sampled in the plane RC of the vessel wall after Nital etching ([10]); (b) : Schematic representation of the segregated zones in the vessel wall

of both alloying elements and impurities [4]. Results presented in Tab.1 are the nominal chemical composition of the A508 class3 steel (BM) and the mean values of the SZ composition, over twenty five analysis. Naudin ([8], [9], [10]) also studied the characteristic size of the SZ's and their spatial

Weight %	C	Mn	Ni	Mo	Cr	Si	Cu	P
BM	0.16	1.35	0.70	0.50	0.19	0.25	0.02	0.008
SZ	0.25	1.88	0.86	1.22	0.22	0.28	0.09	0.025

TAB. 1 – Composition in wt% of BM and SZ materials

distribution. It was found that, with respect to the circumferential frame introduced in Fig.1b, the SZ's are preferentially aligned along A and C directions. A statistical study made over 155 large SZ's (i.e more than 1mm thick) indicates that the average dimensions for a large SZ is $32 \times 16 \times 1.4\text{mm}^3$ (A, C, R), maximum size being $60 \times 59 \times 2\text{mm}^3$. Naudin also studied the influence of the sampling position in the vessel wall. The main result is that when machining a CT_{25} specimen in the inner side of the vessel (distance from the inner side $\in [7; 27\text{mm}]$, case $\boxed{2}$ in Fig.1b) the probability that j SZ's lines intercept the crack front of the CT_{25} follows a Bernoulli law given by :

$$P_j = p^j (1-p)^{n-j} \frac{n!}{j!(n-j)!} \quad (1)$$

where $n = 3$, the mean value (np) being 1.1.

Experimental procedures : For the steel studied, the segregation phenomena taking place during the solidification of ingot produced two materials named BM and SZ (which is homogeneous and representative of the segregated zones) with different mechanical properties. To describe BM material, tensile and compact tensile specimens were sampled in the outer part of the vessel wall (case $\boxed{1}$ in Fig.1b) where the material can be considered as homogeneous and representative of base material. To study the homogeneous SZ material a special ingot has been prepared, its composition being that indicated on Tab.1. Special care was taken to have this « SZ material » as homogeneous as possible. Here again tensile and compact tensile specimens were machined. All the experimental results presented and used hereafter are taken from Naudin studies [8-10].

Mechanical properties : Tensile test have been carried out at four temperatures $[-100, -60, -40, 20]$. The identification of the tensile properties (E Young modulus, σ_0 yield stress, n power law hardening)

was made fitting the tensile test curves with the law :

$$\begin{cases} \epsilon = \sigma/E & \text{for the elastic part } (\epsilon < \epsilon_0) \\ \epsilon_p = \epsilon_0 \left(\frac{\sigma}{\sigma_0}\right)^{1/n} - \frac{\sigma}{E} & \text{for the plastic part } (\epsilon > \epsilon_0) \end{cases} \quad (2)$$

where E is the Young modulus, ϵ_p the plastic strain, n the hardening exponent and ϵ_0, σ_0 constants to be determined. Identification leads to $n_{BM} = 0.122$, $n_{SZ} = 0.112$, $E_{BM} = 215GPa$, $E_{SZ} = 235GPa$, those values are almost independent of the test temperature unlike σ_0^{BM} and σ_0^{SZ} (Fig.2a). For the need of this study, values of σ_0 were extrapolated at other temperatures using Lean model¹ (the filled symbols in Fig.2a). It should be noticed that the ratio $\sigma_0^{SZ}/\sigma_0^{BM}$ tends to increase with temperature.

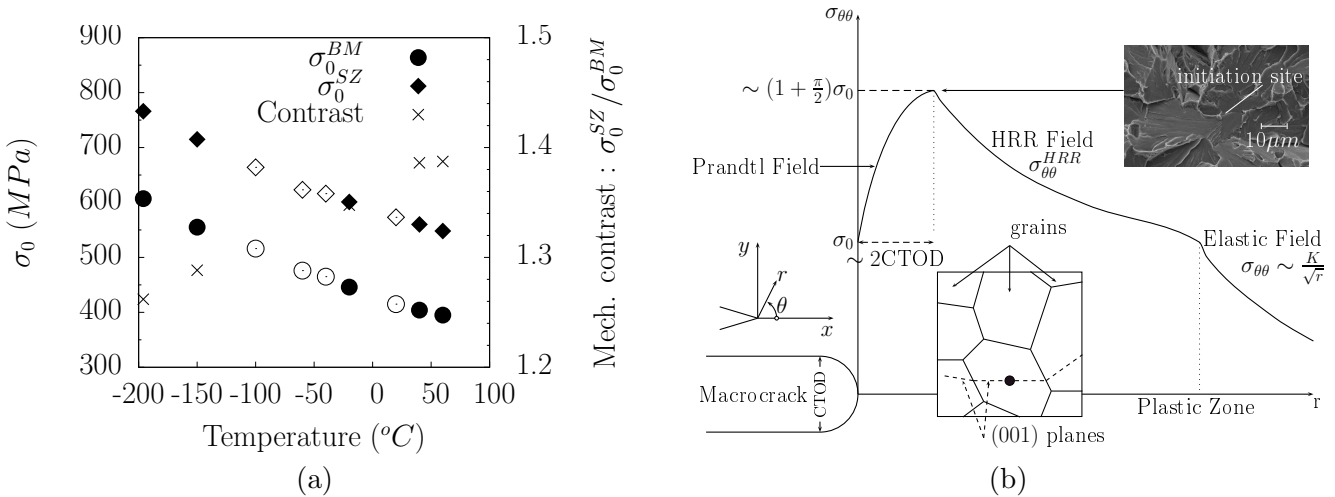


FIG. 2 – (a) : Evolution of σ_0 with temperature for materials BM, SZ ; (b) : Schematic representation of the variations of the tensile stress ahead of a blunted crack tip (SSY conditions)

3 Application of the original Beremin model

Beremin model : The so-called « local approach to fracture » (LAF) for modelling fracture toughness is based on local criteria usually established from tests on volume elements, in particular notched specimens (see e.g., [3], [7]) or precracked specimens. These criteria are applied to the crack tip situation in order to determine the fracture toughness, K_{IC} , provided that the local stress-strain field is known (Fig.2b). The seminal work by Beremin [3] introduced the Weibull stress, σ_w , as a probabilistic fracture parameter and predicts its evolution with the macroscopic applied stress or the stress intensity factor, K , to define the local conditions leading to local material failure. In this approach to brittle fracture the simple axiom is that unstable brittle crack propagation occurs at a critical value of the Weibull stress (for a given failure probability to failure).

The micromechanisms of cleavage fracture in bainitic steels have been described by a number of authors (see e.g. [11], [12]). Here it is enough to say that ahead of a crack tip a number of microcracks are nucleated from defects (carbides, cracks arrested at grain boundaries), as depicted in Fig.2b. Assuming that the defect population follows a power law, the Beremin model leads to a Weibull law expressed as :

$$\ln\left(\frac{1}{1 - P_r}\right) = \frac{B\sigma_0^{m-4}K_I^4 C_{m,n}}{V_0 \sigma_u^m} \quad (3)$$

where K_I is the fracture toughness (K_{IC} or K_{JC}), σ_0 the yield stress, m the Weibull shape factor, $C_{m,n}$ a parameter depending both of the material hardening exponent and the Weibull shape factor (values of $C_{m,n}$ are tabulated in [1]), B the thickness of the specimen, V_0 a representative volume (usually taken equal to the volume of the former austenitic grain) and σ_u the Weibull scale factor.

¹ $\frac{1}{\sigma_0(T)} = \frac{1}{\sigma_0(OK)} + BT$ where B and $\sigma_0(OK)$ are constants and T is the temperature in Kelvin [6]

Application to homogeneous BM and SZ materials : Three K_{JC} data sets are available for the application. Two data sets correspond to the results of compact tensile tests performed on CT_{25} made of homogeneous BM or SZ materials. The third data set corresponds to « real » CT_{25} specimens sampled in the inner part of the vessel shell. The aim of this application is to compare the third data set with the predicted ductile to brittle (DBT) curves of homogeneous BM and SZ materials. Following the methodology proposed for the application of the Beremin model [1], the Weibull parameters describing homogeneous BM and SZ are found to be $\sigma_u^{MB} = 2766 \text{ MPa}\sqrt{m}$, $m_{BM} = 24$, $\sigma_u^{SZ} = 2691 \text{ MPa}\sqrt{m}$, $m_{SZ} = 28$. Applications of the model are shown Fig.3a and Fig.3b, where Δ (resp. \circ) are data obtained on CT specimens made of homogeneous material BM (resp. SZ) and \blacklozenge (resp. \diamond) on CT_{25} specimens sampled close to the inner side of the vessel on which intergranular fracture has been observed at the initiation site (resp. not examined with SEM). Original Beremin model describes accurately the fracture toughness behaviour of the homogeneous material BM (resp. SZ) but not that of specimens sampled close to the inner part of the vessel. It is observed that the Beremin model for homogeneous material tends to overestimate the fracture toughness when the reference is taken as BM material and to largely underestimate the fracture toughness when the reference is the SZ material.

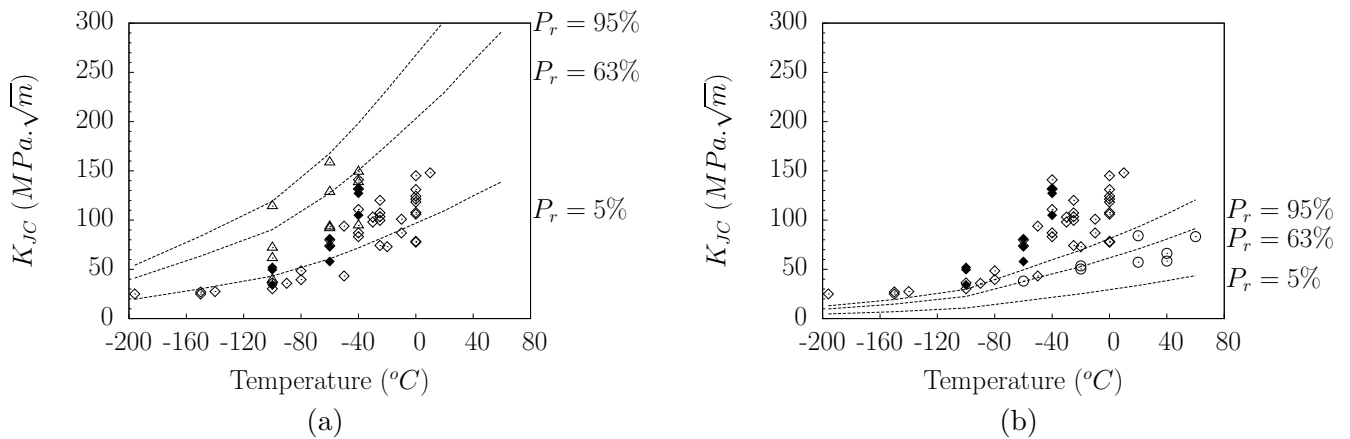


FIG. 3 – Application of the uni-modal Beremin model to : (a) BM ($\sigma_u^{MB} = 2766 \text{ MPa}\sqrt{m}$) , (b) SZ ($\sigma_u^{SZ} = 2691 \text{ MPa}\sqrt{m}$, $m_{SZ} = 28$)

4 Development of bimodal Beremin type model

The aim of this section is to present a model that provides an accurate description of the DBT curve of « real » specimens sampled close to the inner side of the vessel (see Fig.1b).

Main results : 3D simulations were performed to simulate the behaviour of a SZ included in BM material. Details are not presented here. It is enough to say that, although a 1.4mm SZ is inserted in the center of a CT_{25} specimen made of BM material, the crack tip opening displacement ($CTOD$) remains constant along the crack front (except at free surfaces where plane stress conditions prevailed). The $CTOD$ can be approximated by $CTOD = 0.6K^2/(\sigma_0 E)$ thus the iso- $CTOD$ assessment leads to a relation between the stress intensity factor in the BM and that of SZ given by :

$$K_{SZ} = \sqrt{\frac{E_{SZ}\sigma_0^{SZ}}{E_{BM}\sigma_0^{BM}}} K_{BM} \quad (4)$$

Further analysis indicated that as long as the linear fraction of SZ, defined as e_{SZ}/B with e_{SZ} the length of SZ intercepting the crack front, is small (i.e. $< 20\%$) the $CTOD$ of the heterogeneous CT_{25} is equal to that of an homogeneous CT_{25} made of BM. Thus $K_{BM} = K_{macro} = K$ where K is the stress intensity factor of the whole specimen calculated using ASTM standards [2].

Semi-probabilistic description of failure : To introduce the bimodal Beremin model, a simple case is exposed. CT_{25} specimens from the inner side of the vessel are described by their mean com-

position that is to say one SZ of thickness $e = 1.4mm$ intercepts the crack front with a probability of occurrence equal to 100% (the thickness of BM being $B - e$ with $B = 25mm$). Following [13] and using the weakest link theory, the failure probability of the whole specimen, P_r , can be written as :

$$P_r = 1 - (1 - P_r^{BM})(1 - P_r^{SZ}) \quad (5)$$

where P_r^{BM} and P_r^{SZ} are given by :

$$P_r^{BM} = 1 - \exp\left(-\frac{(B-e)K_{BM}^4(\sigma_0^{BM})^{m_{BM}-4}C_{m_{BM},n_{BM}}}{V_0(\sigma_u^{BM})^{m_{BM}}}\right)$$

$$P_r^{SZ} = 1 - \exp\left(-\frac{eK_{SZ}^4(\sigma_0^{SZ})^{m_{SZ}-4}C_{m_{SZ},n_{SZ}}}{V_0(\sigma_u^{SZ})^{m_{SZ}}}\right)$$

Using Eq.4, the probability to failure (Eq.5) can be written as :

$$P_r = 1 - \exp\left(-\frac{(B-e)K^4(\sigma_0^{BM})^{m_{BM}-4}C_{m_{BM},n_{BM}}}{V_0(\sigma_u^{BM})^{m_{BM}}} - \frac{e(E_{SZ}\sigma_0^{SZ}/E_{BM}\sigma_0^{BM})^2K^4(\sigma_0^{SZ})^{m_{SZ}-4}C_{m_{SZ},n_{SZ}}}{V_0(\sigma_u^{SZ})^{m_{SZ}}}\right) \quad (6)$$

Generalisation : When analysing a large number of CT_{25} specimens sampled close to the inner part of the pressure vessel shell and using the distribution given in Eq.1, it appears that the number of large SZ intercepting the crack front varies from 0 to 3. The probability that exactly j SZ's intercept the crack front of a CT_{25} specimen is P_j defined in Eq.1. Assuming that the thickness of a SZ is $e = 1.4mm$ (the average value measured over 155 large SZ's), the probability of failure associated to this case, $P_r(j)$ is given by Eq.6 replacing e by $j \times e$. The probability to failure of the whole specimen, assuming no interaction between the SZ's present along the crack front, is then :

$$P_r = \sum_{j=0}^3 P_j P_r(j) \quad (7)$$

Fracture toughness & scatter predictions : The application of the bimodal Beremin type model described previously, with the determined parameters gives Fig.4a (corresponding to the simplified model with one SZ (Eq.6)) and Fig.4b (corresponding to the generalized model (Eq.7)). In these

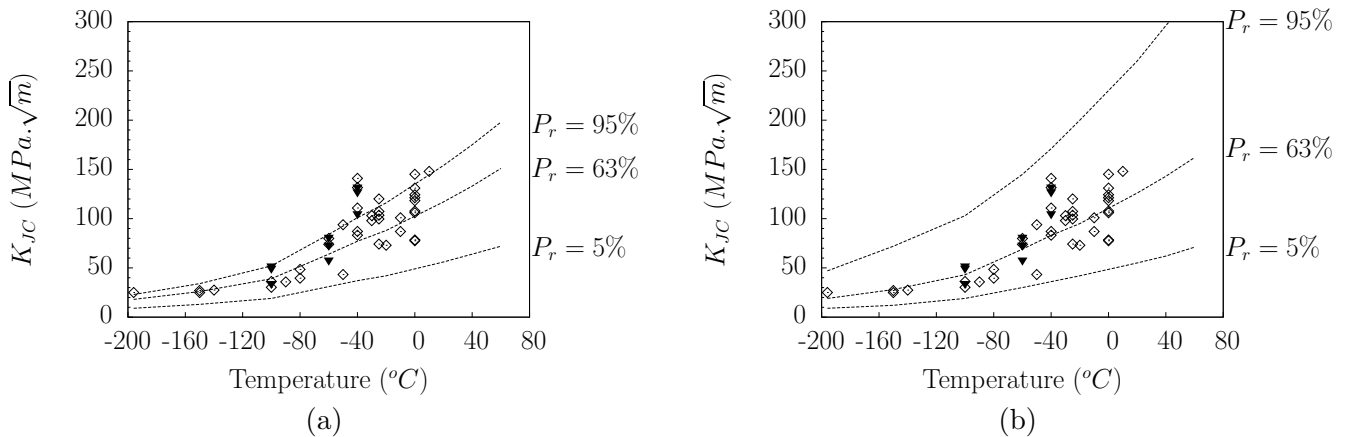


FIG. 4 – Application of the bimodal Beremin type model to the data set corresponding to « real » specimens sampled close to the inner part of the vessel shell (a) simplified model (Eq.6) , (b) generalized model (Eq.7)

figures the filled (resp. open) symbols correspond to test specimens in which the SEM observations confirmed the presence of local intergranular fracture areas in SZ's (resp. the fracture surfaces were not examined). Fig.4a indicates that the assumption of the existence of a single SZ along the crack front is too conservative and underestimates the scatter in results. On the contrary, a much better agreement is obtained when taking the real distribution of SZ (Eq.1).

5 Conclusion

This study has shown that an accurate description of the ductile to brittle transition curve of a real inhomogeneous material is possible using a bimodal Beremin type model (Eq.7), provided that local information such as mechanical properties, failure parameters and the average spatial distribution of inhomogeneities are known. Nevertheless, this model does not account for the interactions between inhomogeneities. This means that the proposed model can only be applied when the volume fraction of inhomogeneities is sufficiently small ($\leq 20\%$). If that volume fraction is exceeded, the model remains unchanged but the simplifying hypothesis $K_{BM} = K_{macro} = K$, as well as the relation between K_{BM} and K_{SZ} have to be reconsidered.

Acknowledgments The experimental part of the present study is taken from C.Naudin thesis (1999). Fruitfull discussions with J.M. Frund and D. Buisine from EDF are gratefully acknowledged. The present study has been made in the frame of the AREVA Professorship with MinesParisTech. Enlightning discussions with P.Joly and F.Roch from AREVA and with J.Besson from MinesParisTech are also acknowledged.

Références

- [1] Andrieu, A., Pineau, A., Besson, J., Ryckelynck, D. 2011 Facilitated implementation of Beremin model : Application to Euro data set *Engineering fracture mechanics, To be published*
- [2] ASTM Standards 2009 ASTM E1820-09 Standard test method for measurement for fracture toughness *American Society of Testing and Materials*
- [3] Beremin, F.M 1983 A local criterion for cleavage fracture of a nuclear pressure vessel steel *Metallurgical and Materials Transactions A* **14(11)** 2277-2287
- [4] Buisine, D. 1989 Influence des zones de ségrégation en éléments d'alliage et en impuretés de types veines sombres sur la résilience d'une pièce forgée en 18MnD5 *Document EDF/EMA : HT-44/PV D 648-A*
- [5] Joyce, J.A., Gao, X. 2002 Analysis of material inhomogeneity in the European round robin fracture toughness data set *Journal of ASTM International* **247** 306-309
- [6] Lean, J.B., Plateau, J., Crussard, C. 1958 Etude des propriétés mécaniques et de la rupture fragile de l'acier doux *C.R. Acad. Sci.* **5(9)** 1-19
- [7] Mudry, F. 1987 A local approach to cleavage fracture *Nuclear Engineering and design* **105(1)** 65-76
- [8] Naudin, C. 1999 Modélisation de la ténacité de l'acier de cuve REP en présence de zones de ségrégation Toughness modelling of PWR vessel steel containing segregation zones PhD thesis HT-42/99/040/A. *EDF - MinesParisTech*
- [9] Naudin, C., Frund, J.M., Pineau, A. 1999 Intergranular fracture stress and phosphorus grain boundary segregation of a Mn-Ni-Mo steel *Scripta Materialia* **40** 9
- [10] Naudin, C., Pineau, A., Frund, JM 2001 Toughness modeling of PWR vessel steel containing segregated zones *10th Conference on Environmental Degradation of Materials in Nuclear Power Systems-water Reactors*
- [11] Pineau, A. 2006 Development of the local approach to fracture over the past 25 years : theory and applications *International Journal of Fracture* **138(1)** 139-166
- [12] Pineau, A., Tanguy, B. 2010 Advances in cleavage fracture modelling in steels : Micromechanical, numerical and multiscale aspects *Comptes Rendus Physique, Ac. Sci.* **11** 316-325
- [13] Tiryakoglu, M., Campbell, J. 2010 Weibull analysis of mechanical data for castings : a guide to the interpretation of probability plots *Metallurgical and materials transactions A* **41(12)** 3121-3129
- [14] Wallin, K., Nevasmaa, P., Laukkanen, A., Planman, T. 2004 Master Curve analysis of inhomogeneous ferritic steels *Engng Fracture Mech.* **71** 2329-2346
- [15] Zhao, X., Lidbury, D., Quinta da Fonseca, J., Sherry, A. 2007 Introducing heterogeneity into brittle fracture modeling of a 22NiMoCr33 ferritic steel ring forging *ASTM special technical publications* **71** 518-539